Solar Energy Materials and Solar Cells 176 (2018) 36–41

Contents lists available at ScienceDirect

Solar Energy Materials and Solar Cells

journal homepage: www.elsevier.com/locate/solmat

Evaluation of thermal physical properties of molten nitrate salts with low melting temperature

Peng Zhang, Jinhui Cheng, Yuan Jin, Xuehui An*

Shanghai Institute of Applied Physics, Chinese Academy of Sciences, Shanghai 201800, China

A R T I C L E I N F O

Keywords:
Molten nitrate salt
Heat transfer fluid
Thermal energy storage
Thermal physical properties

A B S T R A C T

$NaNO_3$-KNO_3 (60–40 wt%, Solar salt) has been used as medium for TES and HTF in the CSP system. One of the key challenges using Solar salt is its high melting temperature, which may freeze and block the pipeline. In this work, a novel eutectic nitrate molten salt of the $LiNO_3$-$NaNO_3$-KNO_3-$CsNO_3$ system with low melting temperature of 368 K is designed using Calphad method. Its thermal physical properties, as well as that of Solar salt, $LiNO_3$-$NaNO_3$-KNO_3, $NaNO_3$-KNO_3-$CsNO_3$, $NaNO_3$-KNO_3-$Ca(NO_3)_2$, and $LiNO_3$-$NaNO_3$-KNO_3-$CsNO_3$-$Ca(NO_3)_2$ molten salts are comprehensively determined and evaluated for better understanding their thermal storage and heat transfer performances, such as the melting temperature, thermal stability, specific heat capacity, thermal diffusivity, density and viscosity. The energy storage capacities and figures of merit of the six molten nitrate salts are calculated based on their thermophysical properties to evaluate their TES and HTF performances. This work not only provides the basic engineering data for CSP system, but is useful for choosing media of TES and HTF.

1. Introduction

Solar energy as a clean and sustainable energy has drawn increasing attention worldwide, but its intermittent energy production has been a challenge for a long time. Concentrated solar power (CSP) plant coupled with storage tank enables continuous energy production even at night or during cloudy days, moreover, it is a reliable electrical power option and carbon free energy production [1]. Medium for thermal energy storage (TES) and heat transfer fluid (HTF) is one of the key techniques because it affects not only the energy production efficiency but also the cost of operation and maintenance of CSP plant [2]. A potential method is to look for a medium with lower melting point and appropriate thermophyscial properties, such as viscosity, density, thermal diffusivity and specific heat capacity [1].

The thermal physical properties of $NaNO_3$-KNO_3, $LiNO_3$-$NaNO_3$-KNO_3 ($LiNaKNO_3$), and $NaNO_3$-KNO_3-$Ca(NO_3)_2$ ($NaKCaNO_3$) systems have been reported by several researchers, especially for $NaNO_3$-KNO_3 system, the mixture of 40 wt% KNO_3-60 wt% $NaNO_3$ (Solar salt), was commercialized as the thermal storage and heat transfer medium in 1937 [3]. Its relatively high melting temperature (~ 493 K) represents an important risk of local solidification and thus block the pipeline during absence of sunshine [4]. Moreover, the investment and operation costs produced by auxiliary facilities of thermal insulation due to high melting temperature are so high that searching for new medium with low melting temperature (lower than 373 K) is necessary. Adding $LiNO_3$, $CsNO_3$, and $Ca(NO_3)_2$ to Solar salt is intended to reduce the melting temperature [5]. A molten salt in the $LiNO_3$-$NaNO_3$-KNO_3-$CsNO_3$-$Ca(NO_3)_2$ ($LiNaKCsCaNO_3$) system was reported to melt at 338 K with a thermal stability over 773 K [6]. We studied the $LiNO_3$-$NaNO_3$-KNO_3-$CsNO_3$ ($LiNaKCsNO_3$) system using the Calphad method and found a novel molten nitrate salt with low melting temperature of 368 K.

Well known, melting temperature is not the only criterion to evaluate TES and HTF medium. Thermal physical properties are also important, such as viscosity, density, specific heat capacity, and thermal diffusivity, because they are the basic and essential engineering data. However, the thermal physical properties are not comprehensively studied in a same work, and the results from different work show discrepancy from each other [7]. For example, the melting temperature of Solar salt is reported to be from 493 to 500 K [8]. The thermal physical properties of $LiNaKNO_3$ system were studied by several researchers, including thermal stability, density, viscosity and specific heat capacity [9–15]. For the $NaKCaNO_3$ system, its thermal physical properties were also reported in Refs. [16,17]. The melting point, stability limit, specific heat capacity, viscosity, density, and thermal conductivity of the nitrate molten salts were summarized in Refs. [10,18]. Although the thermophysical properties of Solar salt, $LiNaKNO_3$ and $NaKCaNO_3$ molten nitrate salts were studied by several researchers, the experimental data are scattered. More important, the thermal diffusivity/conductivity in the liquid state is sparsely available in literatures.

* Corresponding author.
E-mail address: anxuehui@sinap.ac.cn (X. An).

https://doi.org/10.1016/j.solmat.2017.11.011
Received 27 April 2017; Received in revised form 9 November 2017; Accepted 13 November 2017

Table 1
Compositions and cost of the six molten salts.

	Composition (wt%)					Cost (yuan/kg)
	$LiNO_3$	$NaNO_3$	KNO_3	$CsNO_3$	$Ca(NO_3)_2$	
Solar salt		60	40			43.6
$LiNaKNO_3$	30	18	52			144.88
$NaKCsNO_3$		20	24	56		10,771.44
$NaKCaNO_3$		48	36		16	42.8
$LiNaKCsNO_3$	18	12	25	45		8724.58
$LiNaKCsCaNO_3$	8	6	23	44	19	8498.56
Price (yuan/kg)	378	42	46	19,200	38	–

In this work, a novel eutectic molten salt of $LiNO_3$-$NaNO_3$-KNO_3-$CsNO_3$ system with the melting temperature of 368 K is found. The thermophysical properties of Solar salt, $LiNaKNO_3$, $NaNO_3$-KNO_3-$CsNO_3$ ($NaKCsNO_3$), $NaKCaNO_3$, $LiNaKCsNO_3$ and $LiNaKCsCaNO_3$ molten salt systems are systematically and comprehensively determined and evaluated, including melting point, thermal stability, density, specific heat capacity, thermal conductivity, and viscosity. Their thermal energy capacity and figures of merits to evaluate heat transfer capacity are subsequently studied. This work is significant for selection and development of TES and HTF media in the CSP plant.

2. Experimental details

2.1. Sample preparation

The compositions of each molten salts are listed in Table 1. Raw materials of $LiNO_3$, $NaNO_3$, KNO_3 and $CsNO_3$ with purity of 99.9% were separately dried at 473 K under argon atmosphere for 24 h. The mixture of Solar salt was kept at573 K, and the mixture of $LiNaKNO_3$, $NaKCsNO_3$, and $LiNaKCsNO_3$ salt was kept at 473 K for 48 h to make it homogeneous, and then cool down. For $NaKCaNO_3$ and $LiNaKCsCaNO_3$ molten salts, $Ca(NO_3)_2{\cdot}4H_2O$ was used, the raw materials were mixed and transferred in a furnace and heated to 473 K for 48 h, and then heated to 573 K for 72 h to dehydrated.

2.2. Thermal analysis and specific heat capacity

Melting temperatures and specific heat capacities are carried out using the differential scanning calorimeter (DSC, NETZSCH DSC 404 F3). The device was calibrated by six certified reference materials, In, Bi, Sn, Zn, Al, and Au, in the temperature range of 373–1473 K before nitrate molten salts measurement. The extrapolated onset temperature is adopted as the melting temperature, and the peak area is regarded as the melting enthalpy. Both calibration and measurement were finished in the Ar atmosphere flowing at 50 ml/min at the heating rate of 5 K/min.

The specific heat capacities of the six molten nitrate salts in the liquid state were determined using the Ratio method [19]. Two empty high purity graphite crucibles coupled with Pt lids were measured to obtain a baseline. The Pt lid was used to reduce the thermal radiation from furnace. Then, the reference material of monocrystalline sapphire and sample mixtures were subsequently measured using the same crucibles under the same conditions. The specific heat capacity was analyzed by use of Eq. (1), performed automatically using the NETZSCH Proteus program. The uncertainty of specific heat capacity is estimated to be 0.08 J/g K [20].

$$c_{p,S} = \frac{c_{p,R}{\cdot}m_R}{m_S} \times \frac{DSC_S - DSC_B}{DSC_R - DSC_B} \quad (1)$$

Where DSC (μV) is DSC signal, m (g) the mass, c_p (J/g K) the specific heat capacity. B, R and S, are the corresponding parameters of baseline, reference and sample, respectively.

Thermal stability of the molten nitrate salts was determined using the simultaneous thermal analysis (Setaram Labsys Evo TG-DSC) at 10 K/min with the blanket of argon atmosphere, and the flowing rate is also 50 ml/min.

2.3. Determination of density

Density measurements of the Solar salt, $LiNaKNO_3$, $NaKCsNO_3$, $NaKCaNO_3$, $LiNaKCsNO_3$, and $LiNaKCsCaNO_3$ molten salts were realized by a device constructed based on the Archimedes theory. The dimensions of the crucible, platinum cylinder and platinum wire are identified, and the effect of the surface tension on the density has been elaborately discussed in our previous work [20]. The device was calibrated by NaCl and confirmed by LiF-NaF-KF eutectic molten salt [21]. Before measuring the molten nitrate salts density, the volume of a platinum cylinder was calibrated by distilled water at ambient temperature, expressed as Eq. (2)

$$V_0 = \frac{m_0 - m_1}{\rho_w} + \pi D\sigma_w/\rho_w g \quad (2)$$

About 200–300 g molten nitrate salt powder or ingot was melted at target temperature in a furnace with the blanket atmosphere of argon. The platinum cylinder connected to the electronic balance through a platinum wire was completely dipped into the molten salt, and the electronic balance values were recorded at desired temperatures during cooling down at the rate of 1 K/min. The density is calculated by Eq. (3). The uncertainty of density is estimated to be 0.0039 g/cm^3 [21].

$$\rho = \frac{m_1 - m_2 + \pi D\sigma/g}{V_0[1 + \beta(T - 298)]^3} \quad (3)$$

Where ρ is the density, m_0 and V_0 (*ca.* 2.6 cm^3 in our experiment) are the weight and volume of the platinum cylinder in air, respectively; m_1 and m_2 are the weight of the platinum cylinder in distilled water and molten salts, respectively; σ_w and σ are the surface tension of pure water and molten salts, respectively; ρ_w is the density of distilled water; D is the diameter of platinum wire (D = 0.2 mm), g is the gravitational constant; T (K) is the temperature of molten salts; and β is the linear expansion coefficient of platinum ($\beta = 9 \times 10^{-6}$/K).

The surface tension of nitrate salts is usually in 90–120 mN/m [22]. According to Eq. (3), the error caused by surface tension is just 0.00294 and 0.00293 g/cm^3 respectively, when temperature is 473 and 673 K. The uncertainty caused by surface tension is just 0.000245 g/cm^3. The effects of surface tension on the total error (< 0.2%) and uncertainty are very small and can be negligible for nitrate salts.

2.4. Determination of thermal diffusivity

The thermal diffusivities of the Solar salt, $LiNaKNO_3$, $NaKCsNO_3$, $NaKCaNO_3$, $LiNaKCsNO_3$, and $LiNaKCsCaNO_3$ molten salts were measured using the laser flash analysis (Linseis LFA 1000) in helium atmosphere. Sample pretreatment is a key point to determine thermal diffusivity of liquid molten salt using this method. Appropriate amount (about 1.5–2.5 g) of nitrate salt powder was pressed into a disc before it was set in a special designed graphite crucible. The crucible filled with nitrate was heated and kept at a target temperature in a special vacuum furnace for at least half an hour, and then cool down. This heating-cooling under vacuum was repeated 3 times to make the molten salt free from gas bubbles. Finally, the crucible filled with homogeneous molten salt is transferred to the sample cell for thermal diffusivity determination. The molten nitrate salt was kept at each desired temperature for at least 40 min to make temperature homogeneous. The bottom of the crucible was heated by a single laser pulse, and the temperature of front surface was detected by an infrared detector. The temperature rise of front surface with a plot of time was recorded for data analysis, which is finished using the combined model [20,23]. Data analysis was performed automatically using the Evaluation module in the LFEAuto1061 program. The uncertainty of thermal diffusivity is estimated to be less than 15% [20].

2.5. Determination of viscosity

Viscosities of the molten salts were determined using a rotational coaxial cylinder viscometer constructed based on the Brookfield DV-III-series measurement head. This device is feasible to the viscosity of 1.6–20 cP at no more than 1273 K. About 50–100 g nitrate molten salt was put in a graphite crucible with uniform inner diameter of 30 mm and 220 mm in height. The molten salt melted at target temperature for 1 h to make it homogeneous. Then, a special designed inner cylinder with diameter of 26 mm and height of 150 mm was completely dipped into the molten salt in the weight of approximately 100 g. The inner cylinder rotates at the speed of 30 RPM (Revolutions Per Minute) to make sure a laminar flow, and the SMC value was calibrated to be 0.51 by standard viscosity oil. The molten nitrate salts were heated to a target temperature (723 K for Solar salt, and 673 K for other three molten salts), and kept at this temperature for 1 h. A K-type thermocouple is put in the molten salt to measure its temperature accurately. The inner cylinder was driven by a motor, and the torque was recorded. The viscosity of the molten nitrate salt is obtained from Eq. (4). Details are related in our previous work, and the uncertainty of viscosity is estimated to be less than 2.5% [24].

$$\eta = \frac{SMC \times Y\,(torque\%) \times \varepsilon \times 100}{N\,(rpm)} \tag{4}$$

Where η is the viscosity; $SMC = \frac{1}{4\pi(h+c)}(\frac{1}{r^2} - \frac{1}{R^2})$ is a constant related to the dimension of crucible and rotator, and its value is calibrated by standard viscosity oil; h and r represent the length and radius of the rotator; R is the radius of the crucible; c is a constant; SMC calibrated by standard viscosity oil; Y is the torque expressed by percent; ε is a constant; N is the rotating speed.

3. Results and discussion

3.1. Results

For testing the melting temperatures of Solar salt, $LiNaKNO_3$, $NaKCsNO_3$, $NaKCaNO_3$, $LiNaKCsNO_3$, and $LiNaKCsCaNO_3$ molten salts, about 10 mg nitrate salt sample was put in a graphite crucible. The molten salts were heated from room temperature to 523 K for Solar salt, and 473 K for the other five nitrate salts at 5 K/min under the argon atmosphere. The DSC curves of the six nitrate salts are shown in Fig. 1, and the melting peaks are marked as A, B, C, D, E, and F, respectively. For Solar salt, it melts at 495 K, and the melting enthalpy is 87.6 J/g. The melting temperatures of $LiNaKNO_3$, $NaKCsNO_3$, $NaKCaNO_3$, $LiNaKCsNO_3$, and $LiNaKCsCaNO_3$ molten salts are 401, 418, 405, 368, and 351 K, respectively. Obviously, the melting temperature of Solar salt molten salt is lowered by addition of $LiNO_3$, $CsNO_3$, and $Ca(NO_3)_2$, especially the $LiNaKCsNO_3$ and $LiNaKCsCaNO_3$ multi-component molten salts, approximately result in a considerable reduction of 403 and 413 K, respectively. The melting enthalpies are 138.3, 86.0, 5.6, 84.2, and 20.3 J/g, denoting that the enthalpy of molten salt containing $Ca(NO_3)_2$ is too small. The above results tell us that developing multi-component molten salt is an effective method to search novel molten salt with lower melting temperatures.

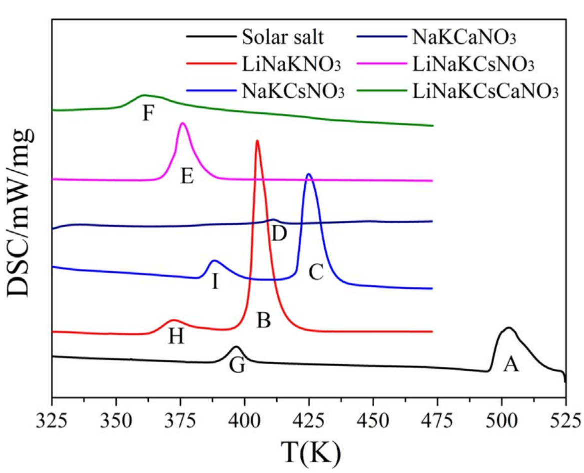

Fig. 1. The DSC curves of the six molten nitrate salts studied in this work.

Actually, two peaks are detected in the DSC curves of Solar salt, $LiNaKNO_3$, and $NaKCsNO_3$, seeing Fig. 1. The small peaks (marked as G–I) are caused by solid transformation, as reported by Olivares et al. [13]. The solid transformation peak will disappear after several re-cycles, which shows satisfied agreement with the results reported in Ref. [25]. In fact, only some mixtures could undergo solid transition, and the transition temperature is also different. These transitions could be observed obviously in DSC curve for the salts whose heat of solid transition is bigger enough, such as Solar salt, $LiNaKNO_3$ and $NaKCsNO_3$. For $NaKCaNO_3$, it's difficult to observe the heat changes caused by solid transition in DSC curve, because that the heat of solid transition is too small. For $LiNaKCsNO_3$ and $LiNaKCsCaNO_3$ with a lower melting point, the salt are melting and the phase become liquid before the solid transition occurs, so it couldn't observe endothermic peak cause by solid transition in DSC curve.

Thermal stabilities of Solar salt, $LiNaKNO_3$, $NaKCsNO_3$, $NaKCaNO_3$, $LiNaKCsNO_3$, and $LiNaKCsCaNO_3$ molten salts are evaluated using thermogravimetric analysis, presented in Fig. 2. The thermal stability limit is defined depended on heating rate, generally, the temperature where the weight loss is 3% at 10 K/min is regarded as the temperature limit [26]. In the present work, the heating rate is 10 K/min, so the temperature when weight loss is 3% (denoted by a black dot line in Fig. 2) is regarded as decomposition temperature. It is 885, 816, 846, 828, 827 and 836 K for Solar salt, $LiNaKNO_3$, $NaKCsNO_3$, $NaKCaNO_3$, $LiNaKCsNO_3$, and $LiNaKCsCaNO_3$ molten salts, respectively. Obviously, the Solar salt is the most stable as temperature increases, and the thermal stability of the multi-component molten salt is lowered. The salt could be used as heat transfer and sensible heat storage material during from melting point to decomposition temperature, and the ΔT (decomposition temperature minus melting point) for the six molten nitrate salts is 390, 415, 428, 423, 459, and 485 K, respectively. This result suggests that Solar salt has the smallest working temperature range although it is the most stable molten salt at high temperature, and the multi-component molten salt with lower melting temperature has a larger working temperature range.

In Fig. 2, the molten nitrate salts gradually decomposed with temperature increasing. Therefore, the thermal properties of the molten nitrate salt in the liquid state were measured below 673 K, since the

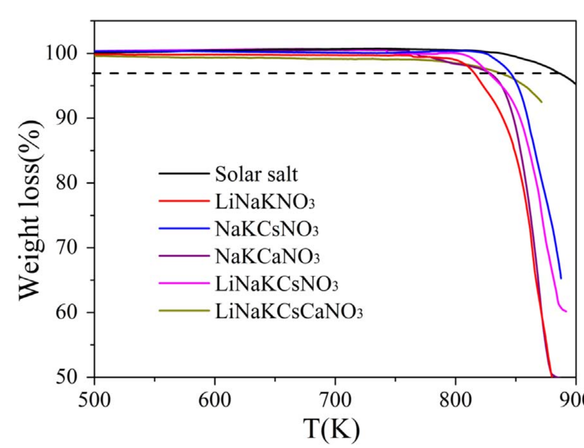

Fig. 2. The TGA curves of the six molten nitrate salts.

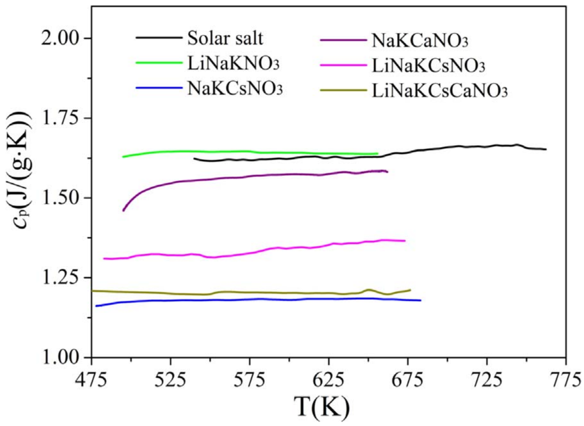

Fig. 3. The specific heat capacities of the six molten nitrate salts the calculated lines.

thermal properties at high temperature are rather similar for different alkali nitrate salt mixtures [27].

The specific heat capacities of the molten salts were determined from Ratio method using DSC. The determination of each molten salt was repeated for three times, and the average values of the last two measurements are adopted, shown in Fig. 3. There is slight change of the specific heat capacities with temperature increasing, so it is reasonable to regard them as a constant, their values are 1.62, 1.65, 1.18, 1.57, 1.32, and 1.20 J/g K corresponding to Solar salt, $LiNaKNO_3$, $NaKCsNO_3$, $NaKCaNO_3$, $LiNaKCsNO_3$, and $LiNaKCsCaNO_3$ molten salts, respectively. The specific heat capacities of Solar salt is obviously decreased by adding $CsNO_3$ and $Ca(NO_3)_2$.

Densities of the molten nitrate salts were determined based on buoyancy of completely immersing a platinum sinker. The buoyancy force can be represented by the weight change read from an electronic balance. A K-type thermocouple was inserted in the molten salt to assure an accurate temperature. The density of the nitrates in the liquid state can be calculated on the basis of the Archimedean principle, and densities of the six nitrate molten salts at different temperatures are shown in Fig. 4. Generally, the temperature dependence of density follows a linear equation, Eq. (5). Therefore, the densities of the molten nitrate salts are regression analyzed, and the parameters in expressions are listed in Table 2. The r^2 of the linear regression equations for the six molten salts are larger than 0.99, indicating an excellent agreement between experimental data and calculated results.

$$\rho = a + bT \tag{5}$$

Where a and b are coefficients calculated based on experimental data.

In Fig. 4, the $NaKCsNO_3$ presents a largest density, the $LiNaKCsCaNO_3$ is secondary, the density of $NaKCaNO_3$ is similar to that of $LiNaKCsNO_3$, which is larger than that of Solar salt, and the density of $LiNaKNO_3$ is smallest. Obviously, the density can be easily increased by adding $CsNO_3$ and $Ca(NO_3)_2$. Actually, the density of the mixture can be calculated by the additive rule [28], so it is related to each single component of the mixture. As we know, the density of $CsNO_3$ and $Ca(NO_3)_2$ is larger than $LiNO_3$, $NaNO_3$ and KNO_3, so the molten salt that contains $CsNO_3$ and $Ca(NO_3)_2$ presents larger density.

Table 2
Coefficients for density and viscosity fitted from experimental data.

	Density		Viscosity		
	a	b (× 10^{-4})	A_0	E_{vis} (kJ/mol)	r^2
Solar salt	2.346	− 7.650	0.1286	15.23	0.986
$LiNaKNO_3$	2.295	− 7.604	0.03337	21.69	0.992
$NaKCsNO_3$	2.861	− 9.713	0.04342	21.21	0.978
$NaKCaNO_3$	2.385	− 7.092	0.05394	21.80	0.998
$LiNaKCsNO_3$	2.438	− 7.906	0.04732	20.57	0.985
$LiNaKCsCaNO_3$	2.788	− 8.723	0.05840	21.64	0.989

Thermal diffusivities of the six molten salts were determined using the laser flash technique verified by H_2O, KNO_3, and LiF-NaF-KF eutectic molten salt, and details were elaborately described in our previous work [20]. The thermal diffusivity of Solar salt is measured from 523 to 673 K with an interval of 50 K. For the $LiNaKNO_3$, $NaKCsNO_3$, $NaKCaNO_3$ and $LiNaKCsNO_3$ molten salts, their thermal diffusivities are determined at the temperature of 473, 523, 573, 623, and 673 K, respectively. Thermal diffusivity of $LiNaKCsCaNO_3$ is measured at 473, 523, 573, and 623 K. At each temperature, the samples are tested for 5 times, and the average value is adopted as the final results, shown in Fig. 5. The thermal diffusivities of the molten nitrate salts slightly increase with temperature increasing below 623 K, however, the thermal diffusivities increase abruptly at 673 K. The phenomenon maybe caused by the structure or volatilization the molten nitrate salts, which is under study and may be clear in the near future. Moreover, we can see that the thermal diffusivity of Solar salt is decreased by addition of $LiNO_3$, $CsNO_3$, and $Ca(NO_3)_2$.

Viscosities of the Solar salt, $LiNaKNO_3$, $NaKCsNO_3$, $NaKCaNO_3$, $LiNaKCsNO_3$, and $LiNaKCsCaNO_3$ molten salts are measured using a self-constructed rotating viscometer. The reliability of the device is confirmed by standard viscosity oil (Cannon S6 oil). The relative deviation from the standard value of Cannon S6 oil was less than 2%, indicating the reliability of the viscometer [24].

The viscosities at different temperatures are presented in Fig. 6. Generally, the temperature dependence of viscosity is described by Arrhenius equation, Eq. (6), and it is adopted in this work. Both the experimental data and the calculated results are shown in Fig. 6. Regression analysis of the viscosity data with Eq. (6) is performed. The calculated parameters, such as A_0, E_{vis}, and r^2, are listed in Table 2,

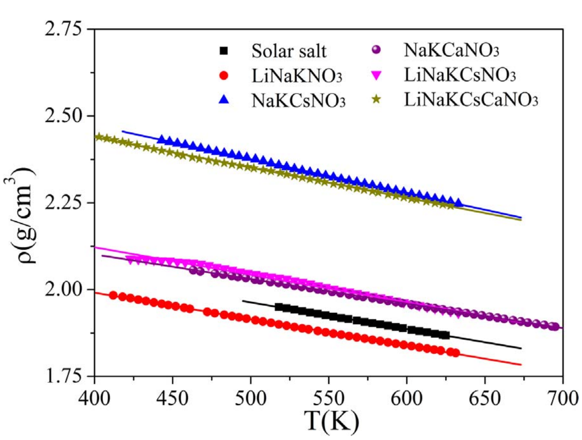

Fig. 4. The densities of the six molten nitrate salts and.

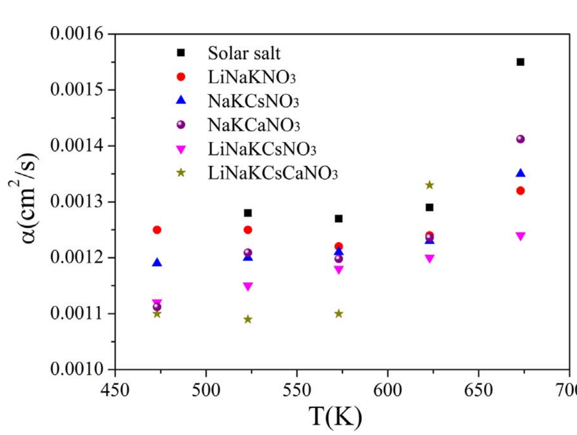

Fig. 5. The diffusivities of the six molten nitrate salts.

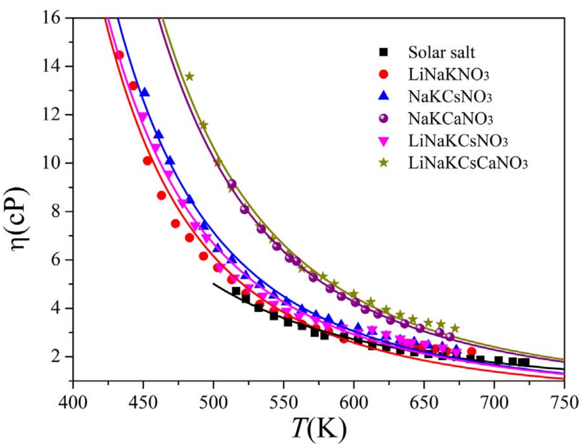

Fig. 6. The viscosities of the six molten nitrate salts and the calculated curves using Arrhenius equation.

which tells us that the least squares correlation coefficients, r^2, are 0.986, 0.992, 0.978, 0.998, 0.985, and 0.989 for Solar salt, $LiNaKNO_3$, $NaKCsNO_3$, $NaKCaNO_3$, $LiNaKCsNO_3$ and $LiNaKCsCaNO_3$ molten salts, respectively. This result indicates that the viscosity of the six molten salts can be well depicted by Arrhenius equation. The calculated activation energy of Solar salt is smallest, 15.23 kJ/mol, and the activation energy of other three molten salts are close to each other, about 21 kJ/mol.

$$\eta = A_0 \exp\left(\frac{E_{vis}}{RT}\right) \tag{6}$$

Where A_0 is a constant, E_{vis} is the activation energy, R is the universal gas law constant.

Seeing Fig. 6, viscosities of $NaKCaNO_3$ and $LiNaKCsCaNO_3$ molten salts are much larger other four molten salts, this may be caused the addition of $Ca(NO_3)_2$. $Ca(NO_3)_2$ presents divalent and is ready to form coordination and increases the viscosity [23]. $LiNaKNO_3$ molten salt shows the smallest viscosity, which may be attributed to the small radius of Li^+, and it is difficult to combine with other ions and decreases the viscosity.

3.2. Discussion

Energy storage density is treated as the most important parameter in the energy storage application because it determines the capacity and efficiency in the heat transfer process. Energy storage density per volume can be calculated by multiplying density, heat capacity and working temperature range. As we know, density is a linear function of temperature, so the energy storage density should be an integral expression, as Eq. (7)

$$E = c_p \cdot \int_{T_m}^{T_{lim}} \rho(T)dT \tag{7}$$

Table 3
The properties and thermal energy storage capacity.

	ρ (g/cm^3)	T_m (K)	T_{lim} (K)	E (J/cm^3)
Solar salt	ρ = 2.346 − 0.0007650T	495	885	1148.61
$LiNaKNO_3$	ρ = 2.295 − 0.0007604T	401	816	1256.38
$NaKCsNO_3$	ρ = 2.861 − 0.0009713T	418	846	1133.82
$NaKCaNO_3$	ρ = 2.385 − 0.0007092T	405	828	1232.19
$LiNaKCsNO_3$	ρ = 2.438 − 0.0007906T	368	827	1190.55
$LiNaKCsCaNO_3$	ρ = 2.788 − 0.0008723T	351	836	1333.23

where E is energy storage capacity, T_m is the melting temperature, T_{lim} is the upper limit of working temperature, which is defined as 3% weight loss in the present work.

The parameters in Eq. (7) are adopted from the present work, listed in Table 3, and the energy storage capacities are calculated to be 1148.61, 1256.38, 1133.82, 1232.19, 1190.55, and 1333.23 J/cm^3 for Solar salt, $LiNaKNO_3$, $NaKCsNO_3$, $NaKCaNO_3$, $LiNaKCsNO_3$, and $LiNaKCsCaNO_3$ molten salts, respectively. Obviously, the $LiNaKCsCaNO_3$ molten salt has the largest energy storage capacity, $LiNaKNO_3$ is secondary, $NaKCsNO_3$ is third, and the energy storage capacity of $NaKCsNO_3$ molten salt is smallest. Actually, many factors have an influence on the energy storage density in practical application.

Figure of merit (FOM), provided by Bonilla [29], is useful to compare the heat-transfer performance of HTF media [27]. FOM for natural and forced convection confirms the superior heat transfer metrics. For forced convection, the FOM is as Eq. (8), while Eqs. (9) and (10) are for natural convection.

$$\text{FOM(forced convection, turbulent)} = \eta^{0.2}/(\rho^2 {c_p}^{2.8}) \tag{8}$$

$$\text{FOM(natural convection, turbulent)} = \eta^{0.2}/(\beta\rho^2 {c_p}^{1.8})^{0.36} \tag{9}$$

$$\text{FOM(natural convection, laminar)} = \eta/(\beta\rho^2 c_p)^{0.5} \tag{10}$$

Where β is the volume expansivity.

FOM is only used for comparison within a group type (salts, metals, or other). Low value of FOM represents better performance. The FOMs of the six molten nitrate salts at 623 K are listed in Table 4, and Solar salt has the smallest FOM values under the natural convection and forced convection, indicating that Solar salt is the best medium as HTF among the six molten salts in this view of point.

Cost is another important point in the commercial application to be considered, so we calculate the cost of the six molten nitrate salts based on price available Sinopharm Chemical Reagent Co. Ltd. in China, listed in Table 1. The cost of $NaKCaNO_3$ is smallest, and Solar salt is secondary, both of which is less than 50 yuan/kg. The molten salts that contain $CsNO_3$ are too much expensive although they have larger working temperature range and larger thermal energy storage capacity.

The melting point is largely decreased by the multi-component molten salt, and it is beneficial to reduce the risk of molten salt freeze and pipe block, as well as the cost of some auxiliary facilities; the large working temperatures of the multi-component molten salt are good for

Table 4
The properties and FOMs at 623 K.

	η (cP)	ρ (g/cm^3)	c_p (J/g K)	β (1/K)	FOM*	FOM#	FOM@
Solar salt	2.39	1.869	1.62	4.09×10^{-4}	8.83×10^{-2}	8.23	32.14
$LiNaKNO_3$	2.51	1.822	1.65	4.17×10^{-4}	8.91×10^{-2}	8.26	33.15
$NaKCsNO_3$	2.85	2.257	1.18	4.30×10^{-4}	15.2×10^{-2}	8.78	33.17
$NaKCaNO_3$	3.51	1.943	1.57	3.65×10^{-4}	9.63×10^{-2}	8.75	40.28
$LiNaKCsNO_3$	2.29	1.941	1.32	4.16×10^{-4}	14.4×10^{-2}	9.07	33.29
$LiNaKCsCaNO_3$	3.94	2.245	1.20	3.89×10^{-4}	15.7×10^{-2}	9.26	40.95

FOM* represents the forced convection, turbulent; FOM# is natural convection, turbulent; FOM@ is natural convection, laminar.

improving the thermoelectric conversion efficiency. However, the cost of the multi-component molten salts is too much higher. In the practical application, the cost of molten salt should be balanced with the thermal storage capacity and heat transfer, which greatly depend on thermal physical properties.

4. Conclusion

In this work, a novel quaternary molten nitrate salt with the melting temperature of 368 K is found using Calphad method. Its thermal physical properties, such as melting temperature, specific heat capacity, thermal diffusivity, density, and viscosity, together with those of Solar salt, $LiNaKNO_3$, $NaKCsNO_3$, $NaKCaNO_3$, and $LiNaKCsCaNO_3$ molten salts are comprehensively studied in this work. The thermophysical properties are the basic input data to calculate thermal energy storage and heat transfer ability, which are evaluated based on the present results. Our results show that the multi-component nitrate molten salt has much lower melting temperature and larger working temperature range, which is benefit to improve the thermal energy storage capacity, but their costs are too much higher. In view of heat transfer performance, Solar salt shows the best among the six molten salts for forced and natural convection.

Acknowledgement

The authors are grateful to acknowledge the financial supported by the National Natural Science Foundation of China (21406256), the “Youth Innovation Promotion Association” (2015214) and “Strategic Priority Research Program” (XD02002400) of Chinese Academy of Sciences.

References

[1] Y.T. Wu, Y. Li, Y.W. Lu, H.F. Wang, C.F. Ma, Novel low melting point binary nitrates for thermal energy storage applications, Sol. Energy Mater. Sol. Cells 164 (2017) 114–121.

[2] Y. Zhao, R.Z. Wang, L.W. Wang, N. Yu, Development of highly conductive KNO_3/$NaNO_3$ composite for TES (thermal energy storage), Energy 70 (2014) 272–277.

[3] W. Kirst, W. Nagle, J. Castner, A new heat transfer medium for high temperatures, Trans. Am. Inst. Chem. Eng. 36 (1940) 371–394.

[4] C. Suarez, A. Iranzo, F.J. Pino, J. Guerra, Transient analysis of the cooling process of molten salt thermal storage tanks due to standby heat loss, Appl. Energy 142 (2015) 56–65.

[5] A.G. Fernández, S. Ushak, H. Galleguillos, F.J. Pérez, Development of new molten salts with $LiNO_3$ and $Ca(NO_3)_2$ for energy storage in CSP plants, Appl. Energy 119 (2014) 131–140.

[6] J.W. Raade, D. Padowitz, Development of molten salt heat transfer fluid with low melting point and high thermal stability, J. Sol. Energy Eng. 133 (2011) 031013-1–031013-6.

[7] R. Serrano-López, J. Fradera, S. Cuesta-López, Molten salts database for energy applications, Chem. Eng. Process.: Process Intensif. 73 (2013) 87–102.

[8] Y. Jin, J.H. Cheng, K. Wang, X.H. An, G.H. Ma, P. Zhang, Z. Li, Research on thermophysical properties of several typical molten salt coolants, Nucl. Tech. 39 (2016) 050604-1–050604-9.

[9] R.W. Bradshaw, Viscosity of multi-component molten nitrate saltstLiquidus to 200 °C, 2010. 〈http://prod.sandia.gov/techlib/access-control.cgi/2010/101129.pdf〉.

[10] N.P. Siegel, R.W. Bradshaw, J.B. Cordaro, A.M. Kruizenga, Thermophysical property measurement of nitrate salt heat transfer fluids, ASME ES2011-54058 (2011) 439–446.

[11] T. Wang, D. Mantha, R.G. Reddy, Thermal stability of the eutectic composition in $LiNO_3$-$NaNO_3$-KNO_3 ternary system used for thermal energy storage, Sol. Energy Mat. Sol. C 100 (2012) 162–168.

[12] T. Wang, S. Viswanathan, D. Mantha, R.G. Reddy, Thermal conductivity of the ternary eutectic $LiNO_3$-$NaNO_3$-KNO_3 salt mixture in the solid state using a simple inverse method, Sol. Energy Mat. Sol. C 102 (2012) 201–207.

[13] R.I. Olivares, W. Edwards, $LiNO_3$-$NaNO_3$-KNO_3 salt for thermal energy storage: thermal stability evaluation in different atmospheres, Thermochim. Acta 560 (2013) 34–42.

[14] K. Coscia, S. Nelle, T. Elliott, S. Mohapatra, A. Oztekin, S. Neti, Thermophysical properties of $LiNO_3$-$NaNO_3$-KNO_3 mixtures for use in concentrated solar power, J. Sol. Energy Eng. 135 (2013) 034506.

[15] D. Mantha, T. Wang, R.G. Reddy, Thermodynamic modeling of eutectic point in the $LiNO_3$-$NaNO_3$-KNO_3 ternary system, J. Phase Equilib. Diffus. 33 (2012) 110–114.

[16] D. Kearney, U. Herrmann, P. Nava, B. Kelly, R. Mahoney, J. Pacheco, R. Cable, N. Potrovitza, D. Blake, H. Price, Assessment of a molten salt heat transfer fluid in a parabolic trough solar field, JSEE (2002).

[17] Y.Y. Chen, C.Y. Zhao, Thermophysical properties of $Ca(NO_3)_2$-$NaNO_3$-KNO_3 mixtures for heat transfer and thermal storage, Sol. Energy 146 (2017) 172–179.

[18] V.M.B. Nunesa, C.S. Queirósb, M.J.V. Lourençob, F.J.V. Santosb, C.A. Nieto de Castrob, Molten salts as engineering fluids – a review: Part I. Molten alkali nitrates, Appl. Energy 183 (2016) 603–611.

[19] ASTM 1269-11 Standard Test Method for Determining Specific Heat Capacity by Differential Scanning Calorimetry.

[20] X.H. An, J.H. Cheng, H.Q. Yin, L.D. Xie, P. Zhang, Thermal conductivity of high temperature fluoride molten salt determined by laser flash technique, Int. J. Heat Mass Transf. 90 (2015) 872–877.

[21] J.H. Cheng, P. Zhang, X.H. An, K. Wang, Y. Zuo, H.W. Yan, Z. Li, A device for measuring the density and liquidus temperature of molten fluorides for heat transfer and storage, Chin. Phys. Lett. 30 (2013) 126501-1–126501-4.

[22] G.J. Janz, Ursula Krebs, H.F. Siegenthaler, R.P.T. Tomkins, Molten salts: volume 3, nitrates, nitrites and mixtures-electrical conductance, density, viscosity and surface tension data, J. Phys. Chem. Ref. Data 1 (3) (1973) 582–746.

[23] L. Dusza, Combined solution of the simultaneous heat loss and finite pulse corrections with the laser flash method, High Temp. High Press. 27 (1995) 467–473.

[24] Y. Jin, J.H. Cheng, X.H. An, T. Su, P. Zhang, Z. Li, Accurate viscosity measurement of nitrates/nitrites salts for concentrated solar power, Sol. Energy 137 (2016) 385–392.

[25] C. Villada, F. Bolívar, F. Jaramillo, J.G. Castaño, F. Echeverría, Thermal evaluation of molten salts for solar thermal energy storage, in: Proceedings of the International Conference on Renewable Energies and Power Quality (ICREPQ'14), 2014. 〈http://www.icrepq.com/icrepq'14/431.14-Villada.pdf〉.

[26] P. Gimeneza, S. Fereres, Effect of heating rates and composition on the thermal decomposition of nitrate based molten salts, Energy Procedia 69 (2015) 654–662.

[27] K. Coscia, S. Neti, A. Oztekin, S. Nelle, S. Mohapatra, T. Elliot, Ternary molten salt heat transfer fluids for energy applications, ASME HT2012-58281 (2012) 249–258.

[28] D. Williams, Assessment of candidate molten salt coolants for the NGNP/NHI heat-transfer loop, 2006. 〈http://csmb.ornl.gov/~webworks/cppr/y2006/rpt/124838.pdf〉.

[29] C. Bonilla, Comparison of coolants, 1958, pp. 9–13.